Effects of rotating noncircular scatterers on spin-wave band gaps of two-dimensional magnonic crystals*

Yang Hui(杨 慧)[a)b)], Yun Guo-Hong(云国宏)[a)b)c)†], and Cao Yong-Jun(曹永军)[a)b)‡]

[a)] College of Physics and Electronic Information, Inner Mongolia Normal University, Hohhot 010022, China
[b)] Inner Mongolia Key Lab of Nanoscience and Nanotechnology, Hohhot 010021, China
[c)] College of Physical Science and Technology, Inner Mongolia University, Hohhot 010021, China

(Received 25 December 2013; revised manuscript received 25 March 2014; published online 13 August 2014)

Using the plane-wave expansion method, the spin-wave band structures of two-dimensional magnonic crystals consisting of square arrays of different shape scatterers are calculated numerically, and the effects of rotating rectangle and hexagon scaterers on the gaps are studied, respectively. The results show that the gaps can be substantially opened and tuned by rotating the scatterers. This approach should be helpful in designing magnonic crystals with desired gaps.

Keywords: magnonic crystal, band gap, rotating, optimizing

PACS: 75.30.Ds, 75.50.Tt, 75.75.–c **DOI:** 10.1088/1674-1056/23/9/097501

1. Introduction

Recently, the magnetic composite materials called magnonic crystals (MCs), have received a great deal of attention because of its remarkable features.[1–25] The most fundamental one is that band gaps exist in the band structures so as to the spin waves in the gaps are forbidden to propagate in the MCs.[1,2] Moreover, people can design band gaps according to their requirements to control the propagations of spin waves in magnonic crystals.[3–6] Meanwhile, this special property will lead to many important potential applications, such as the design of microwave filters,[7] waveguides,[5,8,9] switches,[10] current controlled delay lines,[11] spin-wave logical device,[12] and so on.

Since the spin-wave band gaps is the major feature of MCs, it is essential to tune and optimize the gaps of spin waves propagating in MCs. Thus, most work has been focused on the optimization of the gaps by modulating the magnetic parameters and structural parameters,[13–16] or by changing the external magnetic field.[17] Moreover, there have been also some reports about the modulation of the gaps by changing the damping[18,19] and the interface effects of magnetic materials.[20]

Besides the mentioned above, another important factor preventing the gaps from opening is the degeneracy of spin-wave bands at high symmetry points in the Brillouin zone. The weaker the band degeneracy at high symmetry points is, the easier the gap is formed. It is well known that the degeneracy is lifted by break symmetry of the structure to a certain extent. One method to reduce the structure symmetry is to employ noncircular scatterers, and Cao *et al.*[21] have found that the position and width of the gaps can be tuned and optimized by changing the shape and the arrangement of scatterers arranged in the matrix. Based on the idea mentioned above, we also have tried to reduce the structure symmetry by rotating noncircular, and the results of rotating the square rods show that it really helps to open the gaps through modulating the rotational angles in a certain filling fraction.[22] Mamica *et al.*[23] have investigated the effect of rotating the elliptical rods on the band structure. Recently, Wang *et al.*[24] have presented the other method to reduce the structure symmetry by introducing additional scatterers into each unit cell. The results show that not only for square lattice, but for honeycomb and triangular lattices, the gaps can be improved by introducing additional scatterers. However, to what extent the symmetry should be lowered and what scatterer shape should be rotated can create the largest gaps in a given lattice is not yet known. In this paper, we further consider the effects on band gaps by rotating different noncircular scatterers including rectangle and hexagon rods squarely arranged in a matrix of 2D MCs.

This paper is organized as follows. In Section 2, we briefly describe the model and the method of calculating magnon band structure of 2D MCs. The numerical results are discussed in Section 3. Finally, conclusions are summarized in Section 4.

2. Calculation method and model

Figure 1 shows the cross sections of the 2D MCs and the first Brillouin zone of the square lattice, in which θ is the ro-

*Project supported by the National Natural Science Foundation of China (Grant Nos. 11264028 and 11072104), the Natural Science Foundation of Inner Mongolia Autonomous Region of China (Grant No. 2012MS0114), and the School Scientific Research Funds of Inner Mongolia Normal University of China (Grant Nos. 2013YJRC007 and 2013ZRYB19).

†Corresponding author. E-mail: ndghyun@imu.edu.cn
‡Corresponding author. E-mail: phyjcao@imnu.edu.cn

© 2014 Chinese Physical Society and IOP Publishing Ltd

tational angle, and a is the lattice constant.

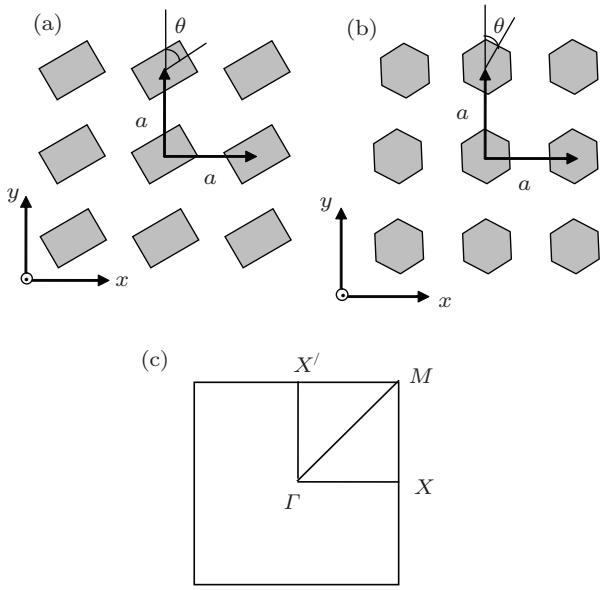


Fig. 1. Cross sections of the 2D MCs with (a) rectangular and (b) hexagon scatterer rods. (c) The first Brillouin zone of the square lattice.

The spin-wave band gaps can be obtained by solving the Landau–Lifshitz equation without a damping term[14]

$$\frac{\partial}{\partial t}\boldsymbol{M}(\boldsymbol{r},t) = -g\boldsymbol{M}(\boldsymbol{r},t)\times\boldsymbol{H}_{\rm eff}(\boldsymbol{r},t), \tag{1}$$

where g is the gyromagnetic ratio ($g>0$) and $H_{\rm eff}$ is an effective magnetic field acting on the magnetization $\boldsymbol{M}(\boldsymbol{r},t)$. When considering short-wavelength perturbations, the magnetostatic term can be neglected compared with the exchange term,[18] and so the effective magnetic field can be described as

$$H_{\rm eff}(\boldsymbol{r},t) = H_0\boldsymbol{z} + \frac{\partial}{\partial \boldsymbol{r}}\left(\alpha_0\frac{\partial}{\partial \boldsymbol{r}}\boldsymbol{M}(\boldsymbol{r},t)\right), \tag{2}$$

where $\alpha_0 = 2A/\mu_0 M_{\rm s}^2$, $M_{\rm s}$, and A are the spontaneous magnetization and exchange constants of ferromagnetic materials, respectively. Both of ferromagnetic materials are assumed to be sufficiently magnetized parallel to the applied magnetic field $\boldsymbol{H}_0$ along the z direction shown in Fig. 1. Magnetization $\boldsymbol{M}(\boldsymbol{r},t)$ can be written as

$$\boldsymbol{M}(\boldsymbol{r},t) = M_{\rm s}\boldsymbol{z} + \boldsymbol{m}(\boldsymbol{r},t), \tag{3}$$

where $\boldsymbol{m}(\boldsymbol{r},t)$ is the dynamic component of the magnetization in the x–y plane, and $|\boldsymbol{m}(\boldsymbol{r},t)| \ll M_{\rm s}$. We also suppose that $m(r,t) = m(r)\,{\rm e}^{-{\rm i}\omega t}$, where ω is the circular frequency of spin wave.

In the process of calculation, we introduce new variables $m_\pm = m_x \pm {\rm i}m_y$, and use the usual linear-magnon approximation of neglecting, in Eq. (1), the small terms of second order in $\boldsymbol{m}(\boldsymbol{r},t)$. It is straightforward to obtain the solution to Eq. (1) with a plane-wave expansion method (PWM)[22]

$$\begin{aligned}\Omega m_{\pm\omega}(\boldsymbol{G}) =& \sum_{G'}[\mu_0 H_0\delta(G-G') + (k+G)\\ &\times(k+G')\alpha(G-G')]m_{\pm\omega}(G'),\end{aligned} \tag{4}$$

where $\Omega = \mu_0\omega/g$, $\alpha = 2A/M_{\rm s}$, and

$$\delta(\boldsymbol{G}-\boldsymbol{G}') = \begin{cases} 1, & \boldsymbol{G}=\boldsymbol{G}', \\ 0, & \boldsymbol{G}\neq\boldsymbol{G}', \end{cases}$$

with $\boldsymbol{G}$ and $\boldsymbol{G}'$ being both the reciprocal lattice vectors.

The Fourier coefficients $\alpha(\boldsymbol{G})$ can be calculated as follows:

$$\alpha(G) = \begin{cases} \alpha_{\rm A}f + \alpha_{\rm B}(1-f), & G=0, \\ (\alpha_{\rm A}-\alpha_{\rm B})P(\boldsymbol{G}), & G\neq 0, \end{cases} \tag{5}$$

where $f = 4l_x l_y/a^2$ and $f = 3\sqrt{3}b^2/2a^2$ are the filling fractions of rectangular and hexagon scatterer rods, respectively. $2l_x$ and $2l_y$ are the length and width of the rectangle, respectively, and b is the edge width of the hexagon. $P(\boldsymbol{G})$ is the structure factor. For the cases of the system with rotational angle θ shown in Figs. 1(a) and 1(b), $P(\boldsymbol{G})$ are respectively expressed as follows:[21]

$$P(\boldsymbol{G}) = f\frac{\sin(\tilde{G}_x l_x)}{\tilde{G}_x l_x}\frac{\sin(\tilde{G}_y l_y)}{\tilde{G}_y l_y}, \tag{6}$$

and

$$P(G) = \begin{cases} \dfrac{2f}{3G_x b}\left[\sin\left(\tilde{G}_x b\right) + \dfrac{1-\cos\left(\tilde{G}_x b\right)}{\tilde{G}_x b}\right], & \tilde{G}_x\neq 0, \tilde{G}_y = 0, \\ \dfrac{f}{3G_x b}\left[\dfrac{1-\cos\left(2\tilde{G}_x b\right)}{2\tilde{G}_x b} + \sin\left(2\tilde{G}_x b\right)\right], & \left|\tilde{G}_x\right| = \left|\tilde{G}_y\right|/\sqrt{3}, \tilde{G}_y\neq 0, \\ \dfrac{f}{G_y b}\left[\dfrac{\cos\left(\frac{\tilde{G}_y b}{\sqrt{3}} - \tilde{G}_x b\right) - \cos\left(\frac{2\tilde{G}_y b}{\sqrt{3}}\right)}{\left(\tilde{G}_y + \sqrt{3}\tilde{G}_x\right)b} + \dfrac{\cos\left(\frac{\tilde{G}_y b}{\sqrt{3}} + \tilde{G}_x b\right) - \cos\left(\frac{2\tilde{G}_y b}{\sqrt{3}}\right)}{\left(\tilde{G}_y - \sqrt{3}\tilde{G}_x\right)b}\right], & \left|\tilde{G}_x\right| \neq \left|\tilde{G}_y\right|/\sqrt{3}, \tilde{G}_y\neq 0, \end{cases} \tag{7}$$

where

$$\begin{cases} \tilde{G}_x = G_x \cos\theta + G_y \sin\theta, \\ \tilde{G}_y = -G_x \sin\theta + G_y \cos\theta. \end{cases} \tag{8}$$

In calculation, we consider the 2D MCs composed of Fe square rods embedded in EuO matrix. For Fe, $A = 2.1 \times 10^{-11}$ J·m^{-1}, $M_s = 1.752 \times 10^6$ A·m^{-1}; and for EuO, $A = 0.1 \times 10^{-11}$ J·m^{-1}, $M_s = 1.910 \times 10^6$ A·m^{-1}. The lattice constant $a = 100$ Å and the applied magnetic field $\mu_0 H_0 = 0.1$ T are chosen in the whole calculation process. In addition, 2601 plane waves are employed in all of the following numerical calculations in order to obtain good convergence.[25]

3. Results and discussion

Now, we study the rectangular scatter rods of 2D MCs shown in Fig. 1(a). First, we consider the case of the ratio between edge widths of the rectangular rods $l_x/l_y = 1.25$. Figure 2 presents the band structures for $\theta = 0°$ and $\theta = 30°$ when the filling fraction $f = 0.5$, respectively. We can easily find that it is similar to the case of rotating square rods[22] that only one band gap appears in the case of $\theta = 0°$ (see Fig. 2(a)), and more calculations also indicate that there is no other gaps except that for any filling fraction under this rotational angle, but two new gaps appear between the higher frequency bands in Fig. 2(b) by rotating the rectangular rods with $\theta = 30°$. It is obvious that the gaps of spin waves will be easily generated by rotating rectangular rods in 2D MCs.

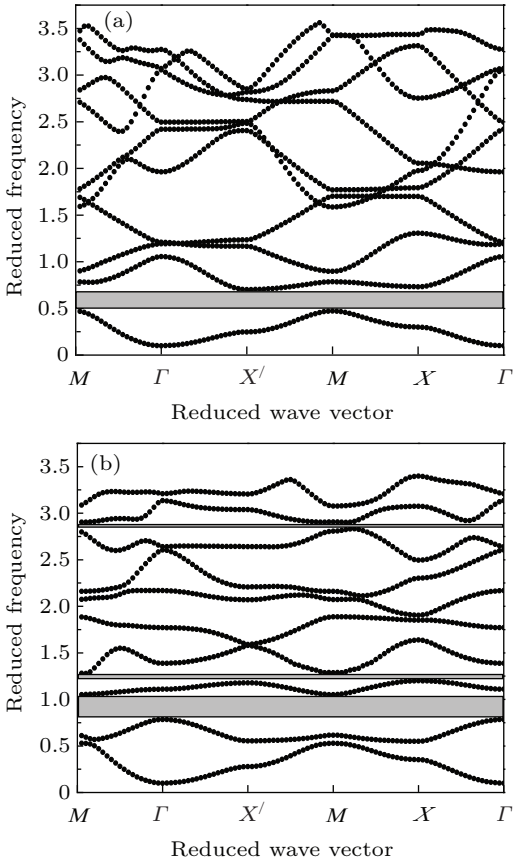


Fig. 2. Spin wave band structures of Fe rectangular rods in EuO at $l_x/l_y = 1.25$ when $f = 0.5$ for (a) $\theta = 0°$ and (b) $\theta = 30°$. The hatched region represents a complete band gap.

We also calculate the dependence of the normalized width $\Delta\Omega/\Omega_g$ of the gap between the second and the third band on the filling fraction f for different rotational angles θ (see Fig. 3), where Ω_g is the frequency in the middle of the gap, and $\Delta\Omega$ the frequency width of the gap. It is notable that when $f < f_{cp}$, f_{cp} is the close-packed filling fraction, and the value of f_{cp} corresponding to θ is given in Table 1. In Fig. 3, one can see that the gap width increases with increasing rotational angle, and the largest normalized gap width $\Delta\Omega/\Omega_g = 0.24259$ when $\theta = 25°$ and $f = 0.6$, which is smaller than the case of square rods which have the same f and θ as the above rectangular rods by comparing with the results of Ref. [22]. This is because for a given lattice symmetry, the same lattice of the geometric symmetry of rod leads to a larger gap width. Thus, the gap width becomes larger by rotating the square rods than by rectangles because the square rods have the same symmetry as the square lattice considered in this paper.

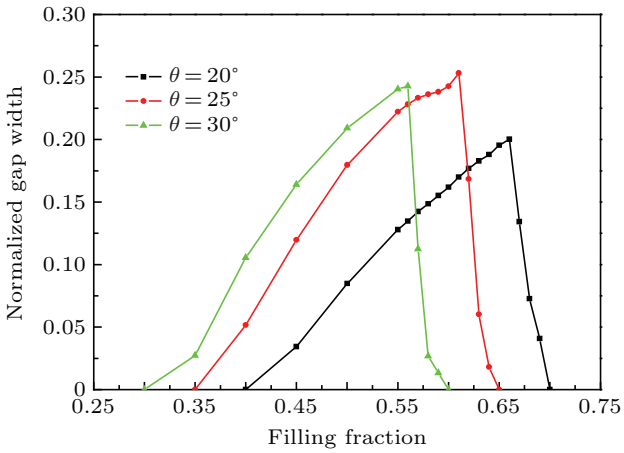


Fig. 3. (color online) Dependence of $\Delta\Omega/\Omega_g$ of the gap between the second and the third band on f for different rotational angles θ.

Table 1. The close-packed filling fraction f_{cp} corresponding to the rotational angle θ.

$\theta/(°)$	$f_{cp} = (l_y/l_x)\cos^2\theta$ [a]		$f_{cp} = (\sqrt{3}/2)\cos^2\theta$ [b]
	$l_x/l_y = 1.25$	$l_x/l_y = 1.4$	
0	0.8	0.714	0.866
5	0.794	0.709	0.859
10	0.776	0.692	0.84
15	0.746	0.666	0.808
20	0.706	0.63	0.765
25	0.657	0.586	0.711
30	0.6	0.536	0.65
35	0.537	0.479	0.581
40	0.469	0.419	0.508
45	0.4	0.357	0.433

[a] f_{cp}: the close-packed filling fraction of rods with rectangular cross.
[b] f_{cp}: the close-packed filling fraction of rods with hexagon cross.

In addition, we also consider another case of the ratio between edge widths of the rectangular rods $l_x/l_y = 1.4$ for a fixed filling fraction $f = 0.5$. The spin-wave band structures at $\theta = 0°$ and $\theta = 30°$ are plotted in Figs. 4(a) and 4(b), respectively. We find only one gap at $\theta = 0°$ as seen in Fig. 4(a). This can also be changed by rotating the rectangular rods shown in Fig. 4(b), and the numbers and the width of gaps increase with increasing rotational angle θ. Moreover, comparing Fig. 4(a) (Fig. 4(b)) with Fig. 2(a) (Fig. 2(b)), we also find that the numbers and the width of gaps decrease as the ratio l_x/l_y increases. The results can be verified by analyzing dependence of the width $\Delta\Omega$ of the gap between the second and the third band on the filling fraction f for different rotational angles θ, as shown in Fig. 5. For $l_x/l_y = 1.0$, the gap width is the largest for either $\theta = 0°$ or $\theta = 30°$. While for other cases at $l_x/l_y > 1.0$, the gap widths at $\theta = 0°$ almost reduce to zero, but the gap widths at $\theta = 30°$ still keep a certain value because the rotating non-circular scatterers would help to open the gaps.

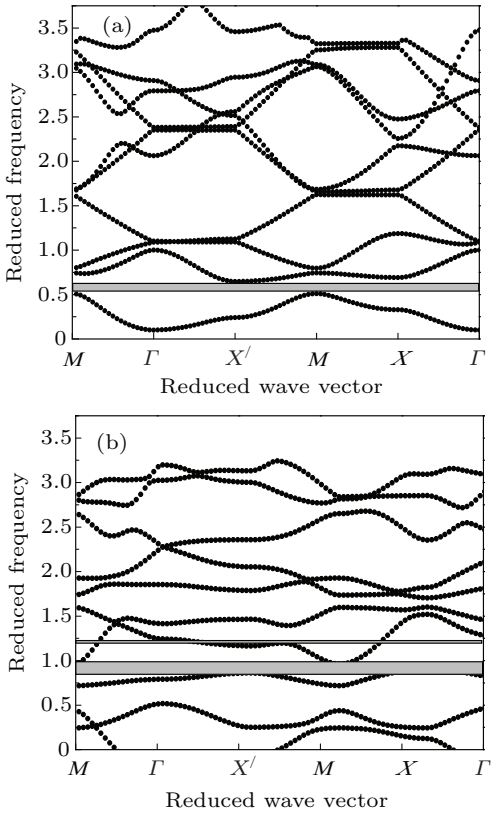


Fig. 4. Spin wave band structures of Fe rectangular rods in EuO at $l_x/l_y = 1.4$ when $f = 0.5$ for (a) $\theta = 0°$ and (b) $\theta = 30°$.

In what follows, the case of hexagonal scatterers in 2D MCs (see Fig. 1(b)) will be considered. When $f = 0.5$, the band structures of 2D MCs with hexagonal scatterers at $\theta = 0°$ and $\theta = 30°$ are displayed in Figs. 6(a) and 6(b), respectively. It can be found that there is only one gap in both cases. Moreover, the width of the gap is almost the same in Figs. 6(a) and 6(b). That is to say, there is almost no influence to gap by rotating hexagonal rods in 2D MCs. This point is different from the cases of square rods and rectangular rods mentioned above. This can be understood that the symmetry of hexagon is higher than square and rectangle, and the symmetry of lattice composed of hexagonal scatterers is broken weaker when rotating the hexagonal rods, so the influence is smaller on gap by rotating the hexagonal rods than the case of rotating the square rods or rectangular rods. In other words, the symmetry of hexagonal rods almost approaches the symmetry of circular rods. The gap of circular rods cannot be absolutely changed by rotating circular rods, because the lattice symmetry of circular rods is not destroyed by rotating circular scatterers.

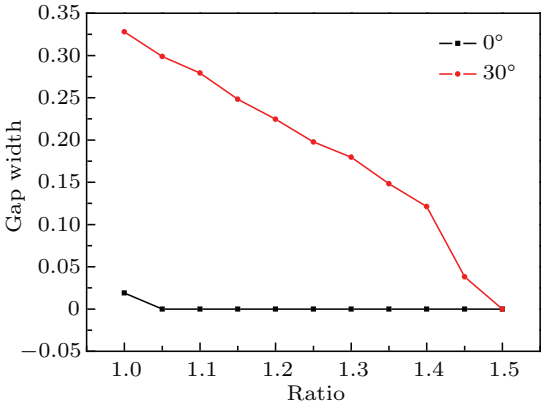


Fig. 5. (color online) Dependence of $\Delta\Omega$ of the gap between the second and the third band on the ratio l_x/l_y for different rotational angles θ.

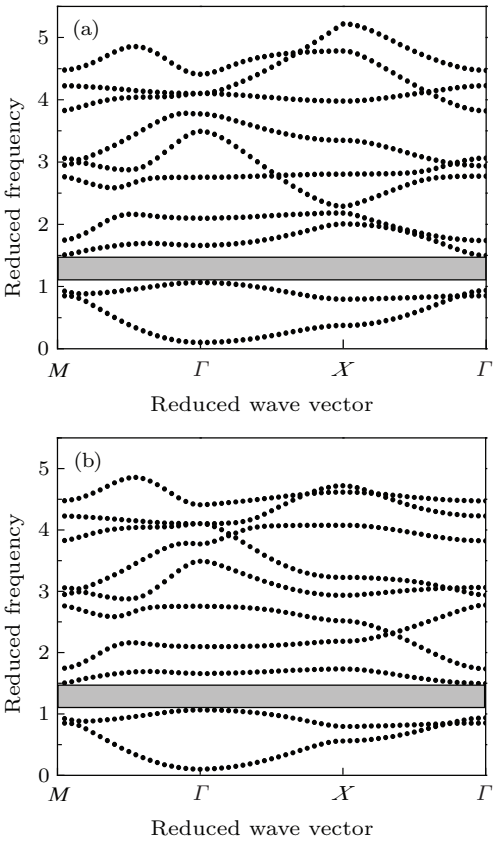


Fig. 6. Spin wave band structure of Fe hexagon rods in EuO at $f = 0.5$ for (a) $\theta = 0°$ and (b)$\theta = 30°$.

Figure 7 shows the numerical results of the normalized width $\Delta\Omega/\Omega_g$ of the gap changes as a function of the filling fraction f for different rotational angles θ, and we can see that the normalized gap width $\Delta\Omega/\Omega_g$ is almost not affected by changing the rotation angle θ except the cases of $0.35 < f < 0.55$. The normalized gap width $\Delta\Omega/\Omega_g$ changes distinctly with increasing rotation angle θ when $0.35 < f < 0.55$, and the largest $\Delta\Omega/\Omega_g = 0.306$ while $\theta = 25°$ and $f = 0.45$. This result indicates that the gap can be optimized by rotating hexagonal scatterers under certain filling fractions, and that the filling fraction f and the rotation angle θ are the collective factors in the optimization of gaps in 2D MCs composed of noncircular scatterers. This point will provide a theoretical basis for the design of gap materials of MCs.

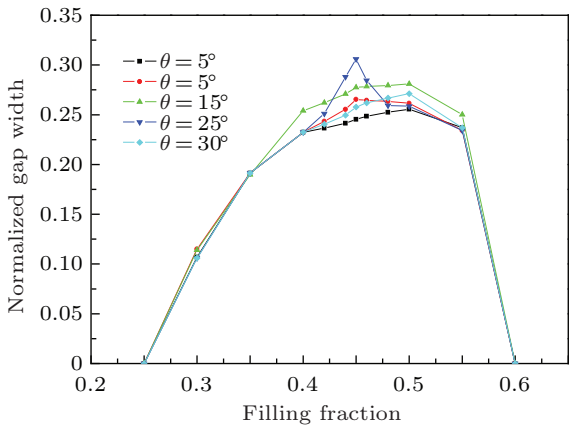


Fig. 7. (color online) Dependence of $\Delta\Omega/\Omega_g$ of the gap on f at different rotational angles θ for hexagon scatterer rods.

4. Conclusion

In this paper, the spin-wave band structures of 2D MCs consisting of Fe scattering rods with different shapes squarely arranged in EuO matrix are calculated using the PWM, and the effects of rotating these noncircular scatterers (rectangle and hexagon) on the band gaps are studied. The results show that the gaps can be substantially opened and tuned by rotating the scatterers. Moreover, the width of the gaps is the largest by rotating the square rods when the rods are squarely arranged in a matrix. For the case of rectangular scatterers, the numbers and width of gaps decrease with the increase in the ratio between edge widths of the rectangle. However, for the case of hexagon scatterers, there is a little influence on the gaps by rotating the scatterers because the symmetry of its own is good enough, but the gaps can be still tuned by rotating the hexagon scatterers with the rotational angles under certain filling fraction. The approach of rotating noncircular scatteres should be very helpful in the design of 2D MCs with desired gaps.

References

[1] Nikitov S A, Tailhades Ph and Tsai C S 2001 *J. Magn. Magn. Mater.* **236** 320
[2] Gubbiotti G, Tacchi S, Madami M, Carlotti G, Adeyeye A O and Kostylev M 2010 *J. Phys. D: Appl. Phys.* **43** 264003
[3] Kruglyak V V, Sokolovskii M L, Tkachenko V S and Kuchko A N 2006 *J. Appl. Phys.* **99** 08C906
[4] Yang H, Yun G H and Cao Y J 2012 *J. Appl. Phys.* **111** 013908
[5] Kim S K, Lee K S and Han D S 2009 *Appl. Phys. Lett.* **95** 082507
[6] Yang H, Yun G H and Cao Y J 2012 *J. Appl. Phys.* **112** 103911
[7] Kim S K, Lee K S and Han D S 2009 *Appl. Phys. Lett.* **95** 082507
[8] Ma F S, Lim H S, Wang Z K, Piramanayagam S N, Ng S C and Kuok M H 2011 *Appl. Phys. Lett.* **98** 153107
[9] Wang Q, Zhong Z Y, Jin L C, Tang X L, Bai F M, Zhang H W and Beach G S D 2013 *J. Magn. Magn. Mater.* **340** 23
[10] Bertotti G, Serpico C, Mayergoyz I D, Magni A, d'Aquino M and Bonin R 2005 *Phys. Rev. Lett.* **94** 127206
[11] Bruno P and Dugaev V K 2005 *Phys. Rev. B* **72** 241302
[12] Kostylev M P, Serga A A, Schneider T, Leven B and Hillebrands B 2005 *Appl. Phys. Lett.* **87** 153501
[13] Vasseur J O, Dobrzynski L, Djafari-Rouhani B and Puszkarski H 1996 *Phys. Rev. B* **54** 1043
[14] Puszkarski H and Krawczyk M 2003 *Solid State Phenom.* **94** 125
[15] Krawczyk M and Puszkarski H 2008 *Phys. Rev. B* **77** 054437
[16] Wang Z K, Zhang V L, Lim H S, Ng S C, Kuok M H, Jain S and Adeyeye A O 2010 *ACS Nano* **4** 643
[17] Wang Z K, Zhang V L, Lim H S, Ng S C, Kuok M H, Jain S and Adeyeye A O 2009 *Appl. Phys. Lett.* **94** 083112
[18] Kruglyak V V and Kuchko A N 2001 *Phys. Met. Metallogr.* **92** 211
[19] Tiwari R P and Stroud D 2010 *Phys. Rev. B* **81** 220403
[20] Tkachenko V S, Kruglyak V V and Kuchko A N 2010 *Phys. Rev. B* **81** 024405
[21] Cao Y J, Yun G H, Liang X X and Bai N S 2010 *J. Phys. D: Appl. Phys.* **43** 305005
[22] Yang H, Yun G H and Cao Y J 2011 *J. Phys. D: Appl. Phys.* **44** 455001
[23] Mamica S, Krawczyk M and Kłos J W 2012 *Advances in Condensed Matter Physics* **2012** 161387
[24] Wang Q, Zhang H W, Tang X L, Su H, Bai F M, Jing Y L and Zhong Z Y 2014 *J. Phys. D: Appl. Phys.* **47** 065004
[25] Cao Y J, Yun G H and Bai N S 2011 *Acta Phys. Sin.* **60** 077502 (in Chinese)